THE ASTROPHYSICAL JOURNAL, 500:1–7, 1998 June 10

THE X-RAY CLUSTER DIPOLE

M. PLIONIS[1] AND V. KOLOKOTRONIS[2]
Received 1997 July 17; accepted 1998 January 20

ABSTRACT

We estimate the dipole of the whole-sky, X-ray flux-limited sample of Abell/Abell, Corwin, & Olowin (ACO) clusters (XBACs) and compare it to the optical cluster dipole, which is known to be well aligned with the cosmic microwave background (CMB) dipole and which converges to its final value at ~ 160 h^{-1} Mpc. We find the X-ray cluster dipole to be well aligned ($\lesssim 25°$) with the CMB dipole, while it closely follows the radial profile of its optical cluster counterpart, although its amplitude is about 10%–30% lower. In view of the fact that the XBAC sample is not affected by the volume incompleteness and the projection effects that are known to exist at some level in the optical parent Abell/ACO cluster catalog, our present results confirm the previous optical cluster dipole analysis that there are significant contributions to the Local Group motion from large distances (~ 160 h^{-1} Mpc). In order to assess the expected contribution to the X-ray cluster dipole from a sample that is closer to being purely X-ray–selected, we compare the dipoles of the XBACs and the brightest-cluster sample in their overlap region. The resulting dipoles are in good mutual agreement with an indication that the XBAC sample slightly underestimates the full X-ray dipole (by $\lesssim 5\%$), while the Virgo Cluster contributes about 12% to the overall X-ray cluster dipole. Using linear perturbation theory to relate the X-ray cluster dipole to the Local Group peculiar velocity, we estimate β_{cx} ($\equiv \Omega_0^{0.6}/b_{cx}$) $\simeq 0.24 \pm 0.05$.

Subject headings: cosmic microwave background — galaxies: clusters: general — large-scale structure of universe — X-rays: galaxies

1. INTRODUCTION

A lively debate has been going on in recent years over the spatial extent of the distribution of mass inhomogeneities that cause the Local Group (LG) motion. Assuming gravitational instability to be the cause of cosmic motions, and using optical and IR galaxies as tracers of the matter distribution, numerous studies (see Yahil, Walker, & Rowan-Robinson 1986; Harmon, Lahav, & Meurs 1987; Lahav 1987; Lahav, Rowan-Robinson, & Lynden-Bell 1988; Lynden-Bell, Lahav, & Burstein 1989; Strauss et al. 1992; Hudson 1993) have shown that most, if not all, of the peculiar acceleration of the LG is induced within 40–50 h^{-1} Mpc. Other analyses of galaxy samples have presented indications of varying strength for contributions from much larger depths, ranging from ~ 100 to ~ 150 h^{-1} Mpc (Plionis 1988; Rowan-Robinson et al. 1990; Plionis, Coles, & Catelan 1993; Basilakos & Plionis 1998). However, the difficulty with such studies in providing a definite answer is that the galaxy samples are not volume-limited but rather magnitude- or flux-limited, which introduces an inherent uncertainty due to the rapid decrease of their selection function with distance from the observer.

On the other hand, being the largest gravitationally collapsed structures in the universe and luminous enough to be volume-limited out to large distances, galaxy clusters have also been used to probe the local acceleration field. Existing studies, all based on the optically selected Abell/Abell, Corwin, & Olowin (1989, hereafter ACO) clusters, provide strong evidence that the LG dipole has significant contributions from depths up to $\sim 160\,h^{-1}$ Mpc (Scaramella, Vettolani, & Zamorani 1991; Plionis & Valdarnini 1991; Tini-Brunozzi et al. 1995; Branchini & Plionis 1996). However, because of the volume incompleteness of richness class $R = 0$ clusters (see Peacock & West 1992), optical projection effects (enhancement of galaxy density along the direction of foreground rich clusters, which cause inherently poor background clusters or groups to appear rich enough to be included in the sample; see Sutherland 1988), and density variations as a function of distance between the Abell and ACO portions of the combined sample (see Plionis & Valdarnini 1991), these results should be verified by well-defined cluster samples, free of such biases.

In the X-ray band, the physical reality of clusters is unquestionable, owing to their strong intracluster medium (ICM) X-ray emission. Two large X-ray cluster samples have been recently compiled: The whole-sky, X-ray flux-limited sample of Abell/ACO clusters (XBACs) was compiled by Ebeling et al. (1996) by carefully cross-correlating the *ROSAT* all-sky X-ray survey (Trümper 1990; Voges et al. 1996) with the Abell/ACO cluster sample; the brightest cluster sample (BCS) was compiled by Ebeling et al. (1997a) from an additional cross-correlation of the *ROSAT* All-Sky Survey (RASS) sources with the Zwicky cluster catalog, but it also contains clusters purely selected in X-rays (for the complete definition see § 2.2). The XBACs sample provides, for the first time, a whole-sky, flux-limited sample of X-ray galaxy clusters suitable for investigating the local acceleration field (for an early attempt using mostly *HEAO 1* data see Lahav et al. 1989). The BCS sample covers only the northern sky, and it has been used to investigate the evolution of the X-ray cluster luminosity function (Ebeling et al. 1997b); both samples will be useful for establishing, among other things, the cluster correlation function (Edge et al. 1998). Nevertheless, both catalogs suffer from some degree of incompleteness at low Galactic latitude (see also §§ 2.3 and 3 for relative corrections). Apart from these two samples, other X-ray cluster samples based on *ROSAT* data are under compilation, most notably the ESO KP catalog

[1] National Observatory of Athens, Lofos Nimfon, Thesio, 18110 Athens, Greece.
[2] Astronomy Unit, School of Mathematical Sciences, Queen Mary and Westfield College, Mile End Road, London E1 4NS, England, UK.

for southern clusters (Collins et al. 1995; de Grandi 1996; Guzzo et al. 1995; Guzzo 1996).

As in the case of all flux-limited samples, the use of these X-ray cluster samples for investigating the very distant contributions to the local acceleration field is limited exactly because of their flux-limited nature. In fact, Kolokotronis et al. (1998) found, using numerical experiments, that such samples will underestimate the true underlying cluster dipole by $\sim 15\%$ on average if distant dipole contributions do exist. We further caution the reader that using clusters to estimate the local acceleration field may be problematic for the following reasons:

1. Because of their large intercluster separation, clusters may not trace the very local gravity field well (~ 30–$40\ h^{-1}$ Mpc) unless the local velocity field is cold, which does seem to be the case (see Peebles 1988); attempts to relate the cluster dipole with the LG peculiar velocity could give erroneous results.
2. Existing cluster samples are incomplete in many different ways. For example, the Virgo Cluster is missing from the optical Abell/ACO catalog and, therefore, also from the XBAC sample. Furthermore, the present X-ray cluster samples may suffer from incompleteness in the nearby universe because of problems in reliably detecting extended low surface brightness emission.

The above limitations will be investigated by comparing the XBACs and BCS dipoles in their overlap region; since the latter sample is closer to being purely X-ray–selected, it has a different luminosity function and lower flux limit, while it also contains the Virgo Cluster.

The outline of this paper is as follows: The X-ray samples and various selection biases are discussed in § 2. The main dipole results are presented in § 3, while in § 4 we estimate the cosmological β parameter. Finally, our main conclusions are presented in § 5.

2. X-RAY SAMPLES AND SELECTION EFFECTS

Both X-ray samples consist of clusters identified in the RASS by a combination of two detection algorithms (the Standard Analysis Software System and Voronoi Tessellation Percolation [SASS and VTP, respectively]) for fluxes above a particular flux limit ($S_{\rm lim}$). The use of the VTP identification algorithm allows quite reliable cluster detections, even at low redshifts, and greatly improves the flux determination for the X-ray sources initially misassessed by SASS (see Ebeling et al. 1996, 1997a and references therein for the superiority of VTP over SASS).

Throughout this work we will be using the following definition of distance (Mattig's formula):

$$r = \frac{c}{H_0\, q_0^2 (1+z)} \left[q_0\, z + (1-q_0)(1-\sqrt{2q_0\, z+1})\right] ,$$

with $q_0 = 0.5$ and $H_0 = 100\, h$ km s^{-1} Mpc^{-1}.

2.1. *XBAC Sample*

The XBACs sample consists of the X-ray brightest Abell/ACO clusters that have been detected in RASS for fluxes above $S_{\rm lim} = 5 \times 10^{-12}$ ergs s^{-1} cm^{-2} (0.1–2.4 keV), with redshifts limited by $z \leq 0.2$. The sample contains 253 clusters, out of which 242 have $|b| \geq 20°$; thus, it is the largest X-ray flux-limited cluster sample to date (though not entirely X-ray selected). The X-ray fluxes measured initially by the SASS point-source detection algorithm are superseded by VTP measurements that account for the extended nature of the emission. In addition, the difficulty of the SASS algorithm in actually detecting nearby X-ray emission has been mostly corrected by running VTP on the RASS fields centered on the optical positions of all nearby Abell/ACO clusters ($z \leq 0.05$), regardless of whether or not they are detected by SASS. Ebeling et al. (1996) estimate, after a careful analysis of possible selection effects and biases, that the overall completeness of this X-ray sample is more than 80%.

2.1.1. *XBAC Systematic Effects*

Because of the cross-correlation of the RASS with the Abell/ACO cluster positions, it is very probable that the systematic biases from which the latter suffer could also creep into the XBAC sample. Ebeling et al. (1996) have shown that the XBAC flux-limited sample is free from the known volume incompleteness as a function of distance of the richness class $R = 0$, Abell/ACO clusters exactly because of the flux-limited property of the XBAC sample, which is such that it contains, at large distances, the inherently brighter, and thus richer, Abell/ACO clusters, for which there is no volume incompleteness.

Another bias from which the optical clusters suffer and which could, therefore, also affect the XBAC sample is the significant distance-dependent density variations between the northern Abell and southern ACO parts of the combined cluster sample (see Batuski et al. 1989; Scaramella et al. 1990; Plionis & Valdarnini 1991). These density variations are most probably due to the higher sensitivity of the ACO IIIa-J emulsion plates, which results in detections of inherently poorer nearby ACO clusters that are missing from the Abell sample. As a first step to quantify the overall magnitude of the effect on the XBAC sample, we estimate, for $|b| > 30°$, the density ratio and its Poisson error between the Abell and ACO parts of the sample within the volume-limited region of the optical cluster sample:

$$\frac{\bar{n}_{\rm ACO}}{\bar{n}_{\rm Abell}}\,(r < 240\ h^{-1}\ {\rm Mpc}) \simeq \begin{cases} 1.56 \pm 0.14\ , & \text{optical}\ , \\ 1.12 \pm 0.17\ , & \text{XBACs}\ , \end{cases}$$

where each cluster has been weighted by $\mathscr{P}(b)(\equiv 10^{\mathscr{A}\ \csc\ |b|})$ to account for the number density decrease due to Galactic absorption.[3] It is evident that X-ray selection has corrected the significant systematic density variation seen in the optical sample. The lower X-ray detection rate of ACO clusters is probably because they are inherently poorer clusters (and thus weaker X-ray emitters), revealed by the higher sensitivity of the IIIa-J emulsion ACO plates.

As already mentioned, the apparent density variations between the Abell and ACO samples are distance-dependent (Plionis & Valdarnini 1991), and, since uncorrected systematic density differences between two parts of the sky can introduce spurious contributions to the dipole, we will statistically correct such variations by weighting each Abell cluster with

$$w(r,\, \delta V_i) = \frac{\bar{n}_{\rm ACO}(r,\, \delta V_i)}{\bar{n}_{\rm Abell}(r,\, \delta V_i)} . \qquad (1)$$

[3] The amplitude of this function has been estimated from each individual cluster sample, and it is consistent with the usually quoted values ($\mathscr{A}_{\rm Abell} \simeq -0.3$ and $\mathscr{A}_{\rm ACO} \simeq -0.2$).

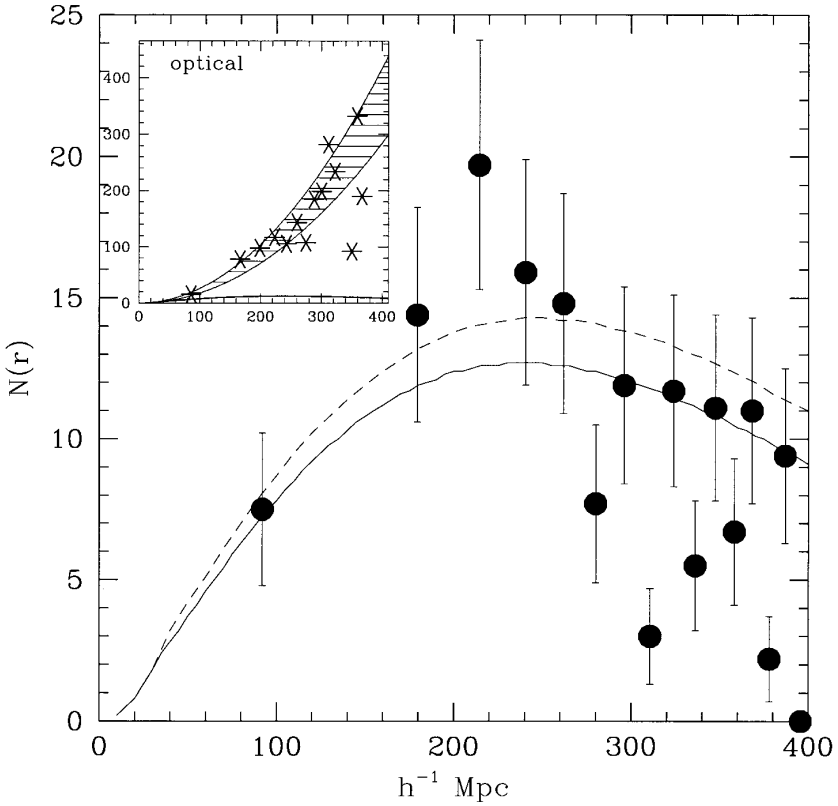

FIG. 1.—Observed $N(r)$ distribution of XBAC clusters, corrected for Galactic absorption, and its Poisson uncertainties. The predicted distribution, via eq. (5), is shown as a solid line. The inset shows the observed $N(r)$ distribution of the optical Abell/ACO clusters (*asterisks*), with the shaded area corresponding to the homogeneous case (i.e., $\phi = 1$) for densities, $\bar{n}_c$, between the Abell and ACO values.

The robustness of our results will be checked by using a large number of bin sizes (δV_i). Note that, because of small-number statistics, the density variations may be insignificant; thus, we will be using $w(r) = 1$ whenever $\sigma(w) \geq |1 - w(r)|$.

2.2. *BCS Sample*

The BCS is the biggest X-ray flux-limited compilation covering the extragalactic sky in the northern hemisphere ($\delta \geq 0°$, $|b| \geq 20°$). It contains 199 clusters above $S_{\rm lim} = 4.45 \times 10^{-12}$ ergs s^{-1} cm^{-2} in the same energy band as the XBACs, with $z \leq 0.3$ and with X-ray luminosities $\geq 1.25 \times 10^{42}\, h^{-2}$ ergs s^{-1}. The BCS sample has been compiled by a cross-correlation of the RASS, not only with the Abell/ACO cluster sample but also with Zwicky clusters, while it also contains clusters selected on the basis of their X-ray properties only. It therefore has a significant overlap with XBACs (for $\delta \geq 0°$) as far as the Abell population is concerned. The above BCS sample is estimated to be 90% complete (redshift completeness is more than 96%).

TABLE 1

PARAMETERS FOR THE XBAC AND BCS X-RAY LUMINOSITY FUNCTION, USING $H_0 = 100\, h$ km s^{-1} Mpc^{-1}

Parameters	XBAC	BCS
A	1.955×10^{-6}	1.246×10^{-6}
α	$1.21^{+0.12}_{-0.13}$	1.85 ± 0.09
L_*	$1.048^{+0.17}_{-0.14}$	$2.275^{+0.515}_{-0.373}$

2.3. *X-Ray Cluster Selection Functions*

In estimating the local acceleration field from flux-limited catalogs, it is necessary to use the sample selection function, which is determined in our case by the cluster X-ray luminosity function, $\Phi_X(L)$. Ebeling et al. (1997b, 1998) have

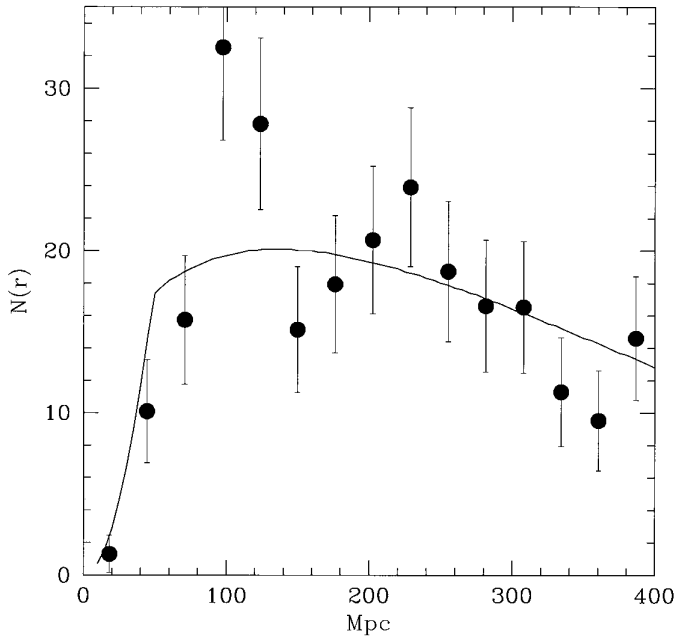

FIG. 2.—Observed $N(r)$ distribution of BCS clusters, corrected for Galactic absorption, and its Poisson uncertainties (*points*). The predicted distribution, via eq. (5), is shown as a solid line.

recently fitted a Schechter-like luminosity function to the data (with parameters given in Table 1):

$$\Phi_X(L) = A \exp\left(-\frac{L}{L_*}\right) L^{-\alpha}, \quad (2)$$

where L_* is the characteristic luminosity measured in 10^{44} h^{-2} ergs s^{-1}, A is the overall normalization of the number density, measured in h^3 Mpc^{-3} $(10^{44}\ h^{-2}$ ergs $s^{-1})^{\alpha-1}$, and α is the usual power-law index.

The selection function, defined as the fraction of the cluster number density that is observed above the flux limit at some distance r, is

$$\phi(r) = \frac{1}{\bar{n}_c} \int_{L_{\min}(r)}^{L_{\max}} \Phi_X(L) dL, \quad (3)$$

with $L_{\min}(r) = 4\pi r^2 S_{\lim}$ and $L_{\max} \simeq 10^{45}\ h^{-2}$ ergs s^{-1} [because of the form of $\Phi_X(L)$, the above integral is very insensitive to larger values of $L_{\max}$]. The mean number density of the underlying X-ray population of clusters is found by integrating the luminosity function from the lower to the upper luminosity limit of the sample:

$$\bar{n}_c = \int_{L_{\min}}^{L_{\max}} \Phi_X(L) dL. \quad (4)$$

Since the absolute lower luminosity limit ($L_{\min}$) is effectively unknown for the XBACs, we can estimate it by relating the above equation with the observed number density of the optical Abell/ACO sample, which can be considered as the "parent" population of the XBAC sample. Using the weighted mean number density of Abell/ACO clusters, corrected for Galactic absorption ($\bar{n}_c \simeq 1.85^{+0.6}_{-0.3} \times 10^{-5}\ h^3$ Mpc^{-3}), we obtain $L_{\min} = 4.3^{+3.5}_{-2.5} \times 10^{41}\ h^{-2}$ ergs s^{-1}: the uncertainty reflecting the density variations between the Abell and ACO samples. For the case of the BCS sample, for which $L_{\min} = 1.25 \times 10^{42}\ h^{-2}$ ergs s^{-1}, we obtain the global mean number density of its parent X-ray cluster population $\bar{n}_c = 5.81 \times 10^{-5}\ h^3$ Mpc^{-3}, a factor of ≈ 3 larger than that of the XBAC sample.

The predicted number of X-ray clusters above $S_{\lim}$ and lying within a shell between r and $r + \Delta r$ is then

$$N(r) = 4\pi r^2 \phi(r) \bar{n}_c \Delta r = 4\pi r^2 \Delta r \int_{L_{\min}(r)}^{L_{\max}} \Phi_X(L) dL. \quad (5)$$

Note that $N(r)$ is independent of $\bar{n}_c$ and thus of the uncertainty in $L_{\min}$. Figure 1 shows the observed number of XBAC clusters as a function of distance and the predicted one from equation (5). The maximum of $N(r)$ turns out to be around $\sim 240\ h^{-1}$ Mpc, in agreement with the observed distribution. If we choose to fit better only the region of reliable redshifts ($\lesssim 0.1$), we would obtain for the luminosity function parameters $\alpha \approx 1.25$ and $L_* \approx 1.2 \times 10^{44}\ h^{-2}$ ergs s^{-1} (Fig. 1, *dashed line*), which, although deviate from the nominal values of Table 1, are within their 1 σ uncertainty. The inset in Figure 1 shows the corresponding $N(r)$ of the optical Abell/ACO cluster, corrected for Galactic absorption (*asterisks*) and the theoretical curve for the range of Abell and ACO densities.

Figure 2 presents the observed BCS $N(r)$ distribution for $|b| \geq 30°$ and the corresponding theoretical one (eq. [5]). The maximum of the selection function turns out to be at $\sim 140\ h^{-1}$ Mpc, followed by a long tail toward larger depths. This early maximum ensures that the BCS function is dominated by relatively local clusters, more so than the corresponding XBAC sample.

Note that we will limit our dipole analysis to the volume within $240\ h^{-1}$ Mpc in order to avoid possible systematic effects due to the low number of the observed X-ray clusters and to uncertainties in the $m_{10} - z$ based cluster redshifts that dominate above this depth.

3. CLUSTER DIPOLE

We will not present all the details of the method used to calculate the peculiar gravitational acceleration induced by some mass tracer on the observer, since such can be found in many recent articles (see Tini-Brunozzi et al. 1995; Kolokotronis et al. 1996 and references therein). Briefly, we employ the method of moments to quantify the distribution of clusters around the LG, and we correct them for the effects of Galactic absorption using a spherical harmonic expansion of the cluster-surface number density and a combined mask to take into account the depletion of clusters for $|b| < 13°$ and a csc b absorption law above this latitude limit (see Plionis & Valdarnini 1991 and the Appendix of Tini-Brunozzi et al. 1995 for details). We then estimate the gravitational acceleration induced in the LG from the distribution of X-ray clusters (see Miyaji & Boldt 1990; Plionis et al. 1993) by

$$\boldsymbol{V}_g(r) = H_0\, r\, \frac{\boldsymbol{D}}{\mathcal{M}}(\leq r) \quad \text{for } r \geq R_{\rm conv}, \quad (6)$$

where $\boldsymbol{D} = \sum \mathcal{W}_i r_i^{-2} \hat{\boldsymbol{r}}_i$ is the dipole, $\mathcal{M} = \sum \mathcal{W}_i r_i^{-2}$ is the monopole, $\mathcal{W}_i$ ($\propto w_i \phi_i^{-1} M_i$) are the cluster weights (with M_i an estimate of the cluster mass), ϕ_i the cluster selection function, and w_i the Abell/ACO relative weight (see eq. [1]). The quantity $R_{\rm conv}$ is the dipole convergence depth, beyond which the distant density inhomogeneities do not affect the dynamics of the observer and should therefore be within the effective depth of the catalog in order to obtain the correct estimate of the local acceleration field. Using the definition of the monopole [$\mathcal{M} = \int \rho(r) r^{-2} dV$] and linear perturbation theory (see Peebles 1980) we can recover from equation (6) the more familiar form

$$\boldsymbol{u}_{\rm LG}(r) = \beta_{c_X} \boldsymbol{D}(r)/4\pi\bar{n}_c = \beta_{c_X} \boldsymbol{V}_g(r), \quad (7)$$

where $\beta_{c_X} \equiv \Omega_0^{0.6}/b_{c_X}$ and b_{c_X} is the X-ray cluster to underlying mass bias factor. Note that we will be using two mass-weighting schemes: one in which we will assume each cluster to contribute equally ($M = 1$) and one in which the mass is proportional to the X-ray luminosity ($M \propto L_X^{5/11}$). This relation results from the assumption of hydrostatic equilibrium, $T \propto M^{2/3}$, and from *ginga* observations, which indicate that $L_X \propto T^{3.3}$ (see Arnaud 1994 and references therein).

However, the sparseness with which the flux-limited sample of clusters trace their underlying parent cluster population introduces shot noise (discreteness effects) in their dipole estimates, which increase with distance. Kolokotronis et al. (1998) used numerical experiments to find that, in cluster distributions that have significant dipole contributions from large depths, the enhancement of the underlying true cluster dipole due to shot noise effects and the loss of dipole signal due to the flux-limited nature of the X-ray sample work in opposite directions, tending to counteract each other. Therefore, although we estimate the magnitude of the one-dimensional shot noise dipole using

the formalism developed in Strauss et al. (1992), i.e., $|\boldsymbol{D}|^2_{\mathrm{sn},1D} \approx \frac{1}{3}\sum \phi_i^{-1} r_i^{-4}(\phi_i^{-1} - 1)$ and find it to be $\sim 30\%$ of the dipole signal, we do not attempt to correct the *raw* XBAC dipole for such effects (for alternative definitions of shot noise see also Hudson 1993; Kolokotronis et al. 1998).

3.1. *Dipole Results*

In Figure 3 we present the cluster dipole (based on both mass-weighting schemes) for the XBAC sample (*triangles*) as well as for the optical Abell/ACO sample (*squares*). It is evident that both samples exhibit a very similar dipole profile, with significant contributions from depths $\gg 100$ h^{-1} Mpc, which validates the previous results based only on the optical sample (Plionis & Valdarnini 1991; Scaramella et al. 1991; Branchini & Plionis 1996). However, the XBAC dipole is systematically lower (by $\sim 20\%$ for the equal mass-weighting case) than the optical cluster dipole. Although this could be intrinsic, implying that the optical dipole is artificially enhanced by projection effects (see Sutherland 1988; Peacock & West 1992), such an explanation is not corroborated by the correlation function analysis of the XBAC sample, which provides a large correlation length, roughly consistent with that of the optical Abell/ACO sample (A. Edge 1997, private communication). An alternative explanation of the lower XBAC dipole amplitude with respect to the optical one is a possibly artificial exclusion from the XBAC catalog of nearby clusters ($\lesssim 50$–60 h^{-1} Mpc), which naturally play a key role in shaping the local acceleration field. In fact, from the eight Abell/ACO clusters within 60 h^{-1} Mpc not included in the XBAC sample, three (A3565, A3574, and A347), although detected in RASS, have been excluded because of suspicion that their X-ray emission is mostly of noncluster origin. If we include these three clusters by hand, then the XBAC ($M = 1$) dipole increases substantially, reducing the difference with the optical dipole from $\sim 20\%$ to $\sim 10\%$. This reduced discrepancy could be further alleviated if we take into account the results of Kolokotronis et al. (1998), who found, using numerical experiments, that the cluster X-ray flux-limited and unity-weighted ($M = 1$) dipole will underestimate the underlying cluster dipole by $\sim 15\%$ if it has significant contributions from large depths ($\gg 100$ h^{-1} Mpc).

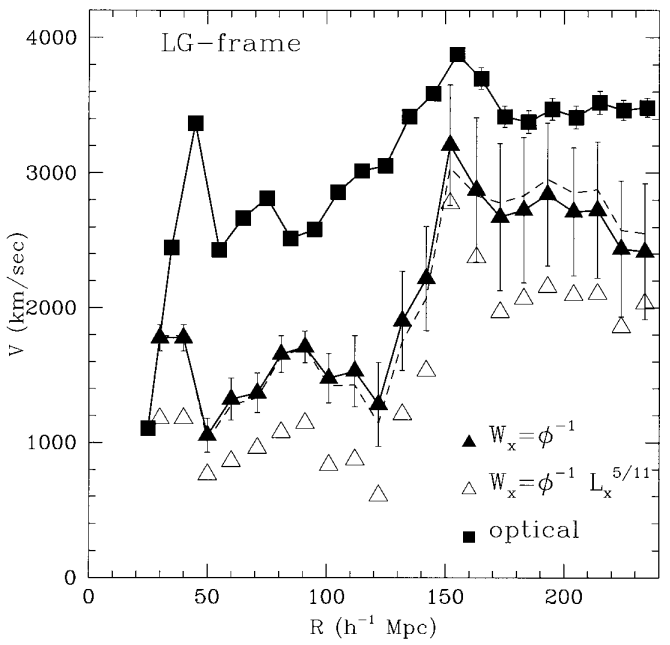

FIG. 3.—Abell/ACO optical (*squares*) and XBAC (*triangles*) dipole. The weighting scheme used is indicated. Error bars are 1 σ uncertainties due to different bin sizes used to homogenize the Abell and ACO number densities (see eq. [1]), while the dashed line is the case with no relative weighting between the Abell and ACO parts of XBACs.

However, using the more natural luminosity-weighting scheme ($M \propto L_X^{5/11}$), we find an even lower amplitude of the XBAC dipole with respect to the unity-weighted one, although their dipole profiles are very similar. The amplitude of the luminosity-weighted X-ray cluster dipole is $\sim 35\%$ less than its optical counterpart, and although the $\sim 25\%$ gap could be bridged, as discussed above, it seems that the X-ray cluster dipole is intrinsically less, by $\gtrsim 10\%$, than the optical cluster dipole. This difference, if it is indeed intrinsic, corresponds to an optical to X-ray cluster bias factor $b_{o,X}(\equiv b_o/b_X) > 1$.

In order to further investigate these points, we will attempt to fill in the lack of local information by using the BCS clusters, which better trace the local volume (see Fig. 2), and compare the XBAC and BCS dipoles in their common region ($\delta > 0°$, $|b| > 20°$). One's hope is that, at the convergence depth of the XBAC dipole, the relative fluctuation between the BCS and XBAC dipoles will reflect those of the whole-sky dipole; therefore, we could infer a better estimate of the final X-ray cluster dipole amplitude.

3.2. *Comparing the XBAC and BCS Dipoles*

The northern XBAC sample (hereafter XBACn) contains 113 clusters, out of which 112 belong to the BCS sample as well, with A2637 being the sole exception (for details see § 10 of Ebeling et al. 1997a). Furthermore, although 65% of the clusters of the two samples are common, it is not obvious that they should similarly trace the northern hemisphere dipole, since (*a*) the BCS is governed by a significantly different $\Phi_X(L)$, which results in a different $N(r)$ distribution (see Figs. 1 and 2), and (*b*) only $\sim 33\%$ and $\sim 53\%$ of the clusters are common within the interesting regions (~ 100 and ~ 200 h^{-1} Mpc, respectively).

For this comparative work, we will correct the raw dipole estimates for shot noise errors, since the two samples should trace the same underlying distribution but with different densities and selection functions. In the lower panel of Figure 4, we plot the fluctuations of the unity-weighted XBACn and BCS dipoles [$\delta V/V \equiv (V_{\mathrm{XBACn}} - V_{\mathrm{BCS}})/V_{\mathrm{BCS}}$] including (*dashed line*) and excluding (*solid line*) Virgo. We also plot (*upper panel*) the misalignment angle between the XBACn and BCS dipoles at each distance bin for the luminosity-weighted one (*solid line*) and for the unity-weighted dipole case (*long-dashed line*), excluding Virgo. The short-dashed line corresponds to the luminosity-weighted dipoles including the Virgo Cluster in the BCS sample.

The most significant results of this analysis are the following:

1. Consistently comparing the BCS and XBACn dipoles (i.e., excluding Virgo from the BCS sample, since by construction it is absent from the XBACs), we find that both X-ray samples have very similar dipole shapes, with small amplitude differences ($\delta V/V \lesssim 0.05$) and $\delta\theta \lesssim 14°$ at scales $\gtrsim R_{\mathrm{conv}}$. Note that the $\delta\theta$ values are uncorrected for the misalignment induced by the shot noise dipole, which is roughly $\sim 10°$.

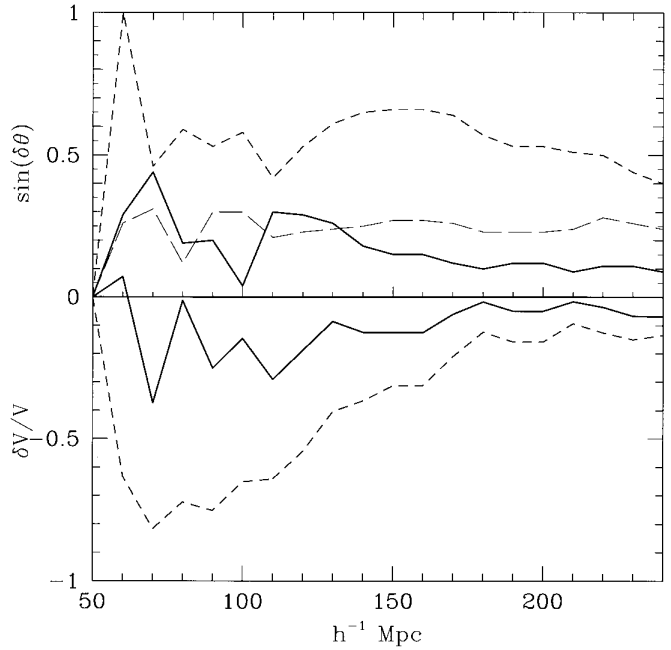

FIG. 4.—Dipole fluctuations ($\delta V/V$) between BCS and XBACn for the unity-weighting scheme excluding (*solid line*) and including (*dashed line*) Virgo. Misalignment angles, $\delta\theta$, with the solid and short-dashed lines corresponding to the L_X-weighted case excluding and including Virgo, respectively. The long-dashed line corresponds to the unity-weighted case, excluding Virgo.

2. If one takes into account the above value of the relative velocity difference between the BCS and the XBACn, one would further reduce the apparent gap between the XBAC all-sky and the optical Abell/ACO dipole, but by not more than $\sim 5\%$.

3. Similarly, with the XBACs and also in the BCS case, the luminosity-weighted dipole is $\sim 20\%$ lower than the corresponding unity-weighted one.

4. Including Virgo in the BCS sample, we find, as expected, that it plays a significant role in shaping the X-ray dipole, with a relative contribution of $\sim 12\%$, which corresponds to an average Virgocentric infall velocity of $\sim 160 \pm 40$ km s^{-1} (where we have twice weighted the luminosity-based results).

4. ESTIMATING THE DENSITY PARAMETER β

The good alignment (within $\sim 25°$) between the XBAC and cosmic microwave background (CMB) dipoles indicates that the XBAC clusters trace the large-scale mass density field and that they can therefore be used to estimate the cosmological β parameter by relating the X-ray cluster dipole to the Local Group peculiar velocity (eq. [7]). However, since the Virgo Cluster is not included in the Abell sample because of its proximity and resulting low surface density, we must exclude the Virgocentric infall from the LG peculiar motion. Equation (7) then becomes

$$\boldsymbol{u}'_{\rm LG} = \boldsymbol{u}_{\rm LG} - \boldsymbol{V}_{\rm inf} = \beta_{c_X} |\, \boldsymbol{V}_g \,| \,. \tag{8}$$

Using $V_{\rm inf} \simeq 170$ km s^{-1}, we find $|\,\boldsymbol{u}'_{\rm LG}\,| \simeq 510$ km s^{-1}, pointing toward $(l, b) = (276°, 16°)$.

The cluster redshift is related to its the comoving distance by

$$cz = H_0 r + [\boldsymbol{v}_p(r) - \boldsymbol{u}_{\rm LG}] \cdot \hat{\boldsymbol{r}} \,, \tag{9}$$

and, since the last term of this equation is not equal to 0, redshift-space distortions (hereafter RSDs) will tend to enhance the dipole amplitude (Kaiser 1987). In an attempt to derive the optical cluster dipole free of such distortions, Branchini & Plionis (1996) used a density reconstruction algorithm to predict the real-space positions of the optical Abell/ACO clusters. They found that RSDs enhance the real-space optical cluster dipole by $\sim 23\%$. In order to correct the XBAC dipole for such effects, we attempt to minimize RSDs, using a simple model of the peculiar velocity field. Since we observe a coherent bulk flow of high amplitude in the local universe (see Dekel 1994, 1997; Strauss & Willick 1995), we split the cluster peculiar velocities into a component of a bulk flow and a local nonlinear component as follows:

$$\boldsymbol{v}_p(r) = \boldsymbol{V}_{\rm bulk}(r) + \boldsymbol{V}_{\rm nl}(r) \,. \tag{10}$$

Applying equation (10) to the Local Group and using equation (8), we have $\boldsymbol{V}_{\rm bulk}(0) = \boldsymbol{u}'_{\rm LG}$, from which it is evident that the bulk flow component locally dominates over that of the infall. This fact may be reversed for galaxies at large distances, but, in any case, at such distances we have $(\boldsymbol{v}_p \cdot \hat{\boldsymbol{r}})/cz \ll 1$; thus, RSDs should not significantly affect the dipole. We therefore use the approximation $\boldsymbol{v}_p(r) = \boldsymbol{V}_{\rm bulk}(r)$, where the bulk-flow profile as a function of distance is given by Dekel (1994, 1997) and by Branchini, Plionis, & Sciama (1996), and its direction is taken to be that of $\boldsymbol{V}_{\rm bulk}(0)$. Note, however, that there have been measurements of the bulk velocity with very different results from the above in direction as well as in amplitude (Lauer & Postman 1994). The reality, however, of these results has been questioned by different studies (see Giovanelli et al. 1996; Hudson & Ebeling 1996).

Our results are completely compatible with those of the full reconstruction of Branchini & Plionis (1996); the redshift-space XBAC dipole is enhanced by $\sim 20\%$ with respect to the corrected (real-space) dipole. The main dipole results and the corresponding values of β_{c_X} (using eq. [7]) are presented in Table 2. Taking into account the probable $\sim 20\%$ artificial decrease of the X-ray dipole (see discussion in § 3.1) and averaging over the different determinations (weighting twice the more physical luminosity-weighted results), we obtain

$$\beta_{c_X} \simeq 0.24(\pm 0.05) \,,$$

where the error bar is not a proper standard deviation (which should also have included the effects of cosmic variance) but rather reflects the uncertainty of the present determination of the mean β_{c_X} value. Note that from the optical Abell/ACO cluster dipole, Branchini & Plionis (1996) found $\beta_{c_o} \approx 0.21$. Furthermore, Branchini et al. (1998), comparing the real-space optical cluster density field

TABLE 2

XBAC DIPOLE PARAMETERS AND THE CORRESPONDING VALUES OF β_{c_X} AT $r = 200\ h^{-1}$ Mpc

Frame	M	$\lvert V_g \rvert$ km s^{-1}	$l°$	$b°$	$\delta\theta_{\rm cmb}$	β_{c_X}
z-Space	1	2710	269	0	17	0.19
z-Space	$L_X^{5/11}$	2100	275	15	19	0.24
Real space.....	1	2250	255	−7	25	0.22
Real space.....	$L_X^{5/11}$	1750	251	10	15	0.29

NOTE.—The value $\delta\theta_{\rm cmb}$ is the dipole misalignment angle from the CMB dipole direction corrected for a 170 km s^{-1} Virgocentric infall.

(within $\sim 70\ h^{-1}$ Mpc) with the corresponding POTENT–Mark III field, found $\beta_{c_o} \approx 0.20 \pm 0.07$. The difference between their β_c value and the present analysis suggests an optical to X-ray cluster bias factor $b_{o,X} \simeq 1.2 \pm 0.4$, a value which is consistent with ≈ 1.

5. CONCLUSIONS

We have estimated the X-ray cluster dipole, using the whole-sky XBAC sample and the BCS sample, which covers the northern hemisphere. We have found the following:

1. The relative contributions to the LG acceleration field from different depths are readily provided by the XBAC dipole analysis and support the conclusions drawn from the optical Abell/ACO cluster analysis of significant dipole contributions ($\sim 30\%$–40% of total) from scales ~ 130–$160\ h^{-1}$ Mpc. Furthermore, the XBAC and BCS clusters trace the same dipole structure equally well and, thus, the large-scale density field.

2. Using a model of the large-scale peculiar velocity field and correcting for RSDs, we find that the real-space X-ray cluster dipole is reduced by $\sim 20\%$, a value consistent with the outcome of a full reconstruction of the optical cluster density field (Branchini & Plionis 1996).

3. Although the "zero point" of the X-ray cluster dipole cannot be unambiguously determined from the present analysis, we find that the true, underlying X-ray cluster dipole is intrinsically lower than the corresponding optical cluster dipole by $\sim 10\%$–30%, depending on whether the X-ray clusters are unity- or luminosity-weighted and on whether one assumes that the observed X-ray emission of a few nearby clusters (A3565, A3574, and A347) is of non-cluster origin.

4. Relating the X-ray cluster dipole with the LG peculiar velocity, we find $\Omega_0^{0.6}/b_{c_X} \simeq 0.24$ (± 0.05), which, if combined with recent determinations based on comparing the optical cluster density and velocity fields with the corresponding POTENT–Mark III fields, suggests a relative optical–to–X-ray cluster bias factor of $b_{o,X} \simeq 1.2 \pm 0.4$.

5. The Virgo Cluster contributes about 12% of the overall X-ray cluster dipole, which corresponds to an average Virgocentric infall velocity of $\sim 160 \pm 40$ km s^{-1}.

We greatly thank Harald Ebeling for many useful discussions, for kindly giving us the XBAC and BCS luminosity functions and the BCS sample prior to publication, and for always meticulously answering our many questions. We also acknowledge fruitful discussions with Alastair Edge on different properties of the XBAC and BCS samples. Finally, we thank Peter Coles for useful comments on the final version of the paper.

REFERENCES

Abell, G. O., Corwin, H. G., & Olowin, R. P. 1989, ApJS, 70, 1
Arnaud, M. 1994, in NATO ASI Ser. 441, Cosmological Aspects of X-Ray Clusters of Galaxies, ed. W. Seitter (Dordrecht: Kluwer), 197
Basilakos, S., & Plionis, M. 1998, MNRAS, in press
Batuski, D. J., Bahcall, N. A., Olowin, R. P., & Burns, J. O. 1989, ApJ, 341, 599
Branchini, E., & Plionis, M. 1996, ApJ, 460, 569
Branchini, E., Plionis, M., & Sciama, D. W. 1996, ApJ, 461, L17
Branchini, E., Plionis, M., Zehavi, I., & Dekel, A. 1998, in preparation
Collins, C. A., et al. 1995, in Wide Field Spectroscopy and the Distant Universe: The 35th Herstmonceux Conference, ed. S. J. Maddox & A. Aragon-Salamanca (Cambridge: World Scientific), 213
de Grandi, S. 1996, in Proc. Int. Conf. on Röntgenstrahlung from the Universe, ed. H. U. Zimmermann, J. Trümper, & H. Yorke (MPE Rep. 263; Würzberg: MPE Rep. 263), 577
Dekel, A. 1994, ARA&A, 32, 371
———. 1997, in Galaxy Scaling Relations: Origins, Evolution, & Applications, ed. L. da Costa (Berlin: Springer), in press
Ebeling, H., Edge, A. C., Böhringer, H., Allen, S. W., Crawford, C. S., Fabian, A. C., Voges, W., & Huchra, J. P. 1997a, MNRAS, submitted
Ebeling, H., Edge, A. C., Fabian, A. C., Allen, S. W., & Crawford, C. S. 1997b, ApJ, 479, L101
Ebeling, H., Voges, W., Böhringer, H., Edge, A. C., Huchra, J. P., & Briel, U. G. 1996, MNRAS, 281, 799
———. 1998, in preparation
Edge, A., et al. 1998, in preparation
Giovanelli, R., Haynes, M. P., Wegner, G., Da Costa, L., Freudling, W., & Salzer, J. J. 1996, ApJ, 464, L99
Guzzo, L. 1996, in Mapping, Measuring, and Modeling the Universe, ed. P. Coles, V. J. Martinez, & Pons-Borderia Maria-Jesus (San Francisco: ASP), 157
Guzzo, L., et al. 1995, in Wide Field Spectroscopy and the Distant Universe: The 35th Herstmonceux Conference, ed. S. J. Maddox & A. Aragon-Salamanca (Cambridge: World Scientific), 205
Harmon, R. T., Lahav, O., & Meurs, E. J. A. 1987, MNRAS, 228, 5
Hudson, M. J. 1993, MNRAS, 265, 72
Hudson, M. J., & Ebeling, H. 1996, ApJ, 479, 621
Kaiser, N. 1987, MNRAS, 227, 1
Kolokotronis, V., Plionis, M., Coles, P., & Borgani, S. 1998, MNRAS, 295, 19
Kolokotronis, V., Plionis, M., Coles, P., Borgani, S., & Moscardini, L. 1996, MNRAS, 280, 186
Lahav, O. 1987, MNRAS, 225, 213
Lahav, O., Edge, A. C., Fabian, A. C., & Putney, A. 1989, MNRAS, 238, 881
Lahav, O., Rowan-Robinson, M., & Lynden-Bell, D. 1988, MNRAS, 234, 677
Lauer, T. R., & Postman, M. 1994, ApJ, 425, 418
Lynden-Bell, D., Lahav, O., & Burstein, D. 1989, MNRAS, 241, 325
Miyaji, T., & Boldt, E. 1990, ApJ, 353, L3
Peacock, J. A., & West, M. J. 1992, MNRAS, 259, 494
Peebles, P. J. E. 1988, ApJ, 332, 17
———. 1980, The Large-Scale Structure of the Universe (Princeton: Princeton Univ. Press)
Plionis, M. 1988, MNRAS, 234, 401
Plionis, M., Coles, P., & Catelan, P. 1993, MNRAS, 262, 465
Plionis, M., & Valdarnini, R. 1991, MNRAS, 249, 46
Rowan-Robinson, M., et al. 1990, MNRAS, 247, 1
Scaramella, R., Vettolani, G., & Zamorani, G. 1991, ApJ, 376, L1
Scaramella, R., Zamorani, G., Vettolani, G., & Chincarini, G. 1990, AJ, 101, 342
Sutherland, W. 1988, MNRAS, 234, 159
Strauss, M. A., & Willick, J. 1995, Phys. Rep., 261, 271
Strauss, M. A., Yahil, A., Davis, M., Huchra, J. P., & Fisher, K. 1992, ApJ, 397, 395
Tini-Brunozzi, P., Borgani, S., Plionis, M., Moscardini, L., & Coles, P. 1995, MNRAS, 277, 1210
Trümper, J. 1990, Phys. Bl., 46(5), 137
Voges, W., et al. 1996, in Proc. Int. Conf. on Röntgenstrahlung from the Universe, ed. H. U. Zimmermann, J. Trümper, & H. Yorke (Würzberg: MPE Rep. 263), 637
Yahil, A., Walker, D., & Rowan-Robinson, M. 1986, ApJ, 301, L1